

Dielectric properties of $\text{Pb}(\text{Co}_{1/3}\text{Nb}_{2/3})\text{O}_3$ under pressure

Tadashi HACHIGA* · Sanji FUJIMOTO · Naohiko YASUDA**

Abstract

The dielectric properties such as the real ϵ' and imaginary ϵ'' parts of the complex permittivity and the spontaneous polarization P_s of single crystal and ceramic $\text{Pb}(\text{Co}_{1/3}\text{Nb}_{2/3})\text{O}_3$ with the diffuse phase transition (DPT) were measured under various pressures up to 6 kbar. The value of ϵ' shows a broad maximum ϵ'_{max} at a temperature T_m (mean Curie temperature). As the pressure increases, the values of ϵ'_{max} and T_m decrease, and the shape of ϵ' around T_m becomes somewhat sharper. The pressure coefficient of T_m is about -3.5 Kkbar^{-1} for the ceramic and -3.0 Kkbar^{-1} for the crystal. Temperature and pressure dependence of ϵ' and P_s is explained in terms of a phenomenological theory using statistical treatments based on a Gaussian distribution of the local Curie temperature. The value of the standard deviation σ describing the intensity of the DPT is 56 K for the ceramic and 47 K for the crystal, and decreases with increasing pressure.

1. Introduction

Recently much attention has been given to the diffuse phase transition (DPT) from points of view of fundamental interest and also of practical importance in the development of ferroelectric materials for capacitor applications¹⁾. Complex perovskite type ferroelectrics with disordered cation arrangements generally show DPT which is characterized by a broad maximum for the temperature dependence of the permittivity and a large deviation from the Curie-weiss law in a wide temperature range around the transition point. Lead cobalt niobate $\text{Pb}(\text{Co}_{1/3}\text{Nb}_{2/3})\text{O}_3$ is a perovskite ferroelectric exhibiting DPT. The structure is cubic at room temperature²⁾. In this compound the octahedral sites of the crystal are occupied randomly by Co^{2+} and Nb^{5+} ions²⁾. Malkov and Venevtsev have indicated that there are large differences in the values of the transition point T_t (or mean Curie temperature θ_{av}) for a single crystal and ceramic sample³⁾. The effects of the d.c. bias on the dielectric properties have been reported as a function of temperature for the

* Takayama Junior College

** Gifu University

single crystal $\text{Pb}(\text{Co}_{1/3}\text{Nb}_{2/3})\text{O}_3$ with DPT⁴⁾. On the other hand, little has been reported on the pressure dependence of the dielectric properties of $\text{Pb}(\text{Co}_{1/3}\text{Nb}_{2/3})\text{O}_3$. In this paper, the temperature and pressure dependence of the dielectric properties such as the real and imaginary parts of the complex permittivity, the spontaneous polarization and the mean Curie temperature of $\text{Pb}(\text{Co}_{1/3}\text{Nb}_{2/3})\text{O}_3$ are presented and explained in terms of a phenomenological theory, using statistical treatments based on a Gaussian distribution of the local Curie temperature.

2. Experimental Method

All the specimens were prepared from the starting materials PbO (purity > 99.999%, particle size < 1 μm), CoO (purity > 99.9%, particle size < 1 μm), Nb₂O₅ (purity > 99.9%, particle size < 1 μm). The intimate mixtures were ballmilled with acetone for a day, then dried and pressed into a disc. The discs were calcinated in N₂ atmosphere at 800°C for 4h^{5,6)} (then an excess of PbO must be provided in the crucible in order to compensate for PbO evaporation). The resulting cake was reground, pressed into pellets, and refired at 950°C for 4h in a controlled PbO and N₂ atmosphere in a Pt crucible. Powder x-ray diffraction of this reacted powder showed a simple cubic perovskite structure. All the ceramic specimens were prepared by usual ceramic techniques which has been described elsewhere^{7,8,9)}. The reacted powders were pulverized to fine powders (particle size < 0.5 μm), and then pressed into a disc under a pressure of about 2000 kgcm⁻². The discs were sintered at 980°C for 4h in a controlled PbO and N₂ atmosphere in a Pt crucible. X-ray powder patterns of ceramic specimens showed cubic powder patterns of the perovskite type (lattice constant $a = 4.045 \text{ \AA}$) at room temperature, as reported previously³⁾. Grain sizes were a few microns. The apparent density of the ceramics was 95 to 97% of the theoretical density (8.48 gcm⁻³)²⁾. Single crystals for dielectric study were grown from the PbO flux by the slow cooling technique¹¹⁾. The weight ratio of the flux to the reacted powders of $\text{Pb}(\text{Co}_{1/3}\text{Nb}_{2/3})\text{O}_3$ was 4 : 1. The thermal cycle used was a rapid heating to 1150°C, soaking at that temperature for 4h, cooling at 3°C/h to 900°C, 5°C/h to 800°C and then 50°C/h back to room temperature. The crystals were separated from the excess PbO by boiling in 20~30 percent nitric acid solution. These crystals have the form of simple cubes with well developed 100 faces. Figure 1 shows the crystal of $\text{Pb}(\text{Co}_{1/3}\text{Nb}_{2/3})\text{O}_3$. The crystal growings were also tried with the flux of PbO-PbF₂ used in the ratio by weight PCNO : PbO : PbF₂ = 1 : 4 : 4, the results were not improved, compared with the case of PbO only. X-ray diffraction and dielectric studies confirm that the specimen prepared for this study is the single phase. X-ray powder patterns of single crystal $\text{Pb}(\text{Co}_{1/3}\text{Nb}_{2/3})\text{O}_3$ at room tempera-

ture showed cubic powder patterns of the perovskite type (lattice constant $a=4.046 \text{ \AA}$, as reported previously²⁾. The lapped specimen was electroded with silver paste (Dupont No 7075) by firing at 590°C for 5 min. The electrical capacitance and the dielectric loss tangent were measured at 100KHz with a field of less than 5Vcm^{-1} using an AC bridge, and the spontaneous polarization was examined with a Sawyer-Tower circuit. The 60Hz AC electric field was applied to the

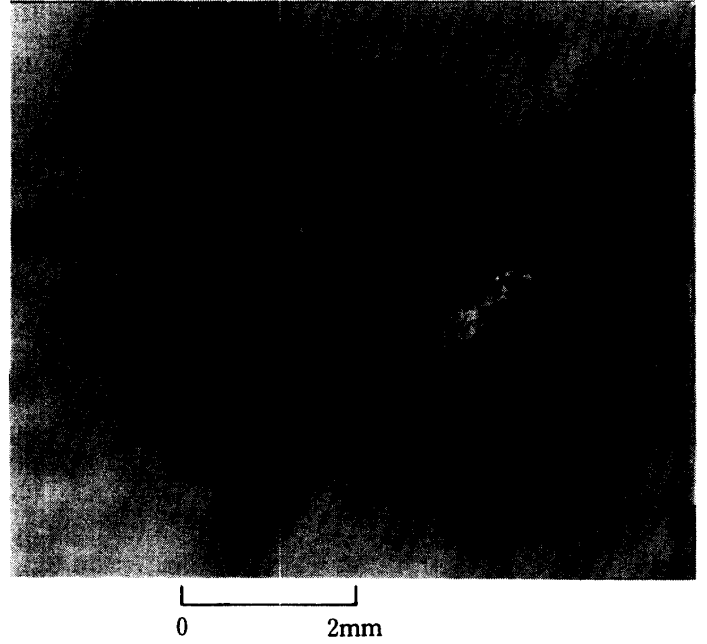


Figure 1. $\text{Pb}(\text{Co}_{1/3}\text{Nb}_{2/3})\text{O}_3$ single crystals

specimen as pulses for only 1 s. A Cu-Be pressure vessel with a pressure-transmitting fluid (1 : 1 mixture of n- and iso-pentane) was used to apply the pressure to the specimen¹²⁾. The pressure was measured with manganin gauges to an accuracy of $\pm 1.5\%$ and the temperature to within $\pm 0.1^\circ\text{C}$ with a calibrated Cu-constantan thermocouple. All the dielectric data were collected while increasing the temperature at a rate of 0.2 Kmin^{-1} at various constant pressures, and all of the data observed were reversible, with good reproducibility, when the pressure was lowered.

3. Experimental results

Figures 2 and 3 show the temperature dependence of the real part ϵ'_r and the imaginary part ϵ''_r of the complex relative permittivity of single crystal and ceramic $\text{Pb}(\text{Co}_{1/3}\text{Nb}_{2/3})\text{O}_3$ at 100KHz for different pressures. The small AC field was applied along [001] for the single crystal. The values of ϵ'_r for both samples show a broad maximum at a temperature T_m , which is characteristic of DPT. Figure 4 shows the pressure dependence of the temperature T_m at the maximum in ϵ'_r and the value of the maximum in ϵ'_r ($\epsilon'_{r\text{max}}$). The dielectric behavior is qualitatively similar between ceramic and single crystals. As the pressure increases, the value of T_m and the value of the $\epsilon'_{r\text{max}}$ for both samples decrease as shown in figure 4. The value of T_m for the single crystal is smaller than that for the ceramic, and such a fact has been indicated by Malkov and Venevtsev³⁾. For both samples, T_m decreases linearly with pressure with slopes $(dT_m/dp) \approx -3.5 \text{ Kkbar}^{-1}$ for the ceramic and -3.0 Kkbar^{-1} for the crystal. The pressure coefficient of T_m for the ceramic is larger

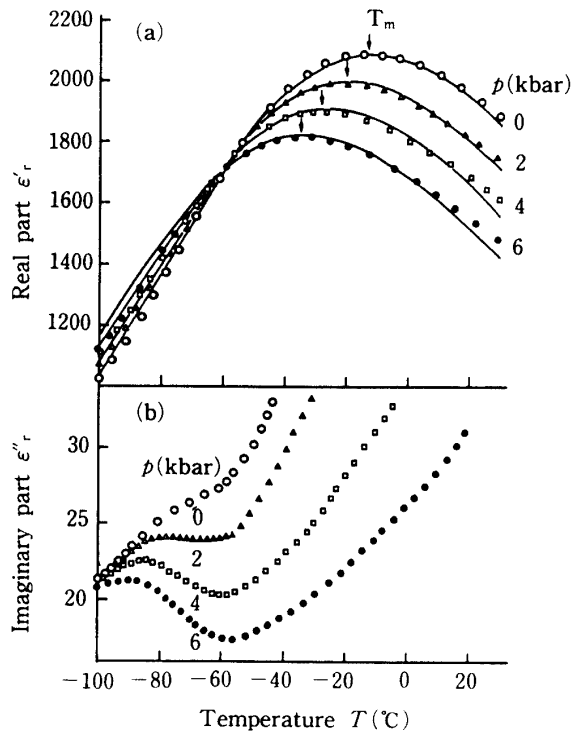


Figure 2. Temperature dependence of (a) the real ϵ'_r and (b) the imaginary ϵ''_r part of the complex relative permittivity of ceramic $\text{Pb}(\text{Co}_{1/3}\text{Nb}_{2/3})\text{O}_3$ at 100KHz for different pressures. Full curves are calculated values.

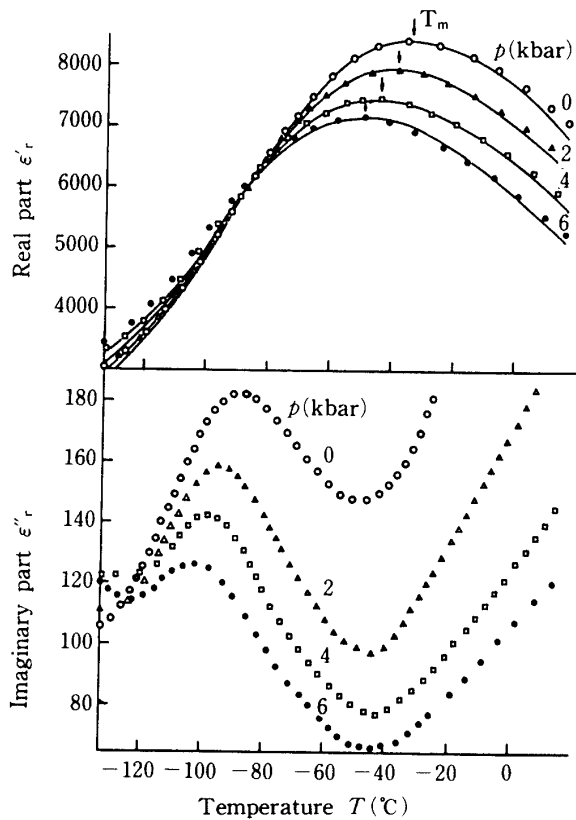


Figure 3. Temperature dependence of (a) the real ϵ'_r and (b) the imaginary ϵ''_r part of the complex relative permittivity of crystal $\text{Pb}(\text{Co}_{1/3}\text{Nb}_{2/3})\text{O}_3$ at 100KHz for different pressures. Full curves are calculated values.

than that for the single crystal. These values are comparable with values of -3.8 Kkbar^{-1} for the ceramic and -3.6 Kkbar^{-1} for the single crystal of disordered $\text{Pb}(\text{Sc}_{1/2}\text{Ta}_{1/2})\text{O}_3$ with DPT¹³⁾, respectively. The value of ϵ''_r shows a maximum at a temperature lower than T_m , and then shows a minimum with increasing temperature. The rapid increase in ϵ''_r with T at temperatures above about -40°C is due to the increase in the conductivity with T . With increasing pressure, the maximum in ϵ''_r shifts towards lower temperatures, while the minimum in ϵ''_r shifts towards higher temperatures. These anomalies in ϵ''_r for

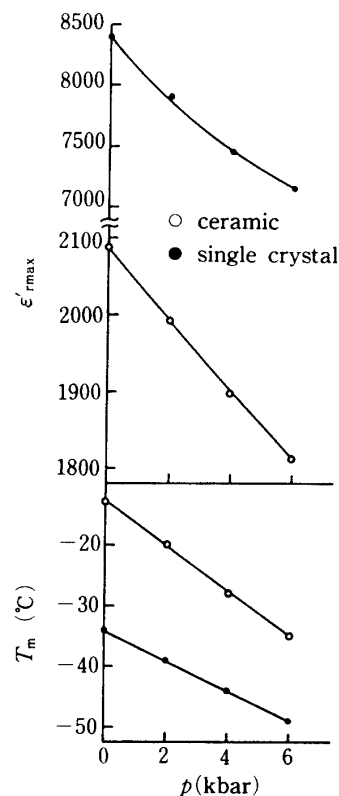


Figure 4. Pressure dependence of the maximum value of ϵ'_r ($\epsilon'_{r\text{max}}$) and the temperature T_m that gives $\epsilon'_{r\text{max}}$.

both samples are enhanced with increasing pressure. The anomaly and its enhancement with increasing pressure for the single crystal are greater than that for the ceramic.

The permittivity of ferroelectrics with the DPT deviates greatly from the Curie-Weiss law at temperatures above the transition point T_t (or mean Curie temperature θ_{av} ; see § 4). Empirically the relative permittivity at temperatures above T_t has been known to be described by the following relation :

$$\frac{1}{\epsilon'_r} - \frac{1}{\epsilon'_{r\max}} = \frac{(T - T_m)^\gamma}{C'} \quad (1)$$

where C' is the Curie-like constant and γ is the critical exponent^{14,15}. The value of γ is nearly unity (Curie-Weiss behaviour) for the sharp phase transition such as BaTiO_3 ^{14,15}. $\gamma=2$ for ferroelectrics where DPT has been derived theoretically on the basis of a microscopic composition-fluctuation model¹⁶. The correlation between the critical exponent γ and the phase transition diffuseness has been pointed out by Uchino and Nomura¹⁵. Figure 5 shows logarithmic plots of the reciprocal relative permittivity ($1/\epsilon'_r - 1/\epsilon'_{r\max}$) at 100KHz against the reduced temperature ($T - T_m$) of the single crystal for different pressures. It is found from the linearity of the curves in figure 5 that equation (1) holds good for different pressures. The slope of the straight line decreases with increasing pressure. The values of the critical exponent γ determined from its slope and the Curie-like constant C' estimated from equation (1) decrease with increasing p as shown in the inset in figure 5. The values of γ and C' for the crystal are 1.85 and 7.1×10^7 , respectively, at atmospheric pressure. These values are comparable with values of 1.64 and 1.4×10^7

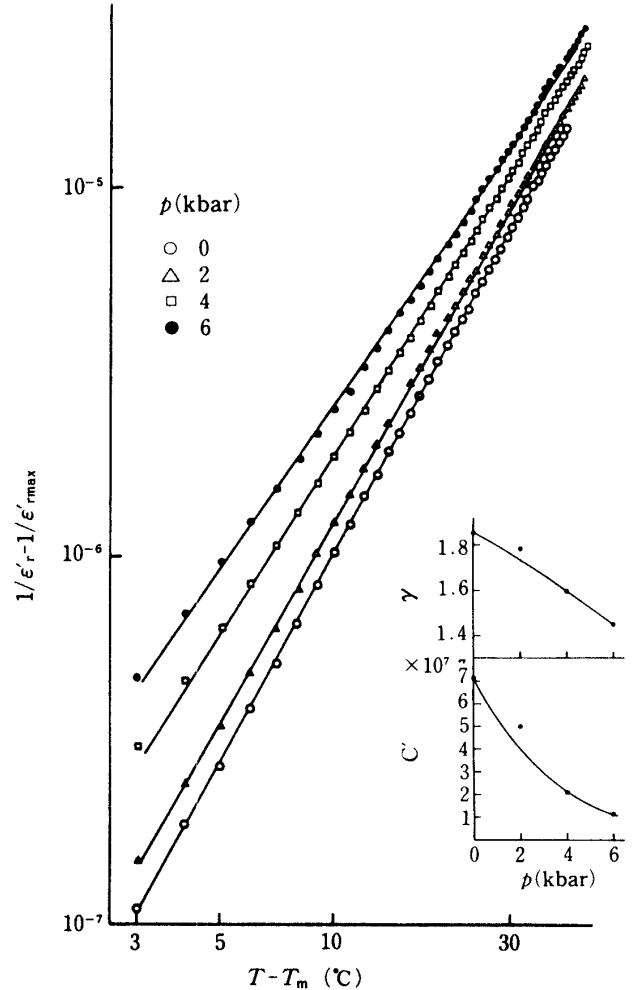


Figure 5. Logarithmic plots of the reciprocal relative permittivity ($1/\epsilon'_r - 1/\epsilon'_{r\max}$) at 100KHz against the reduced temperature ($T - T_m$) of single crystal $\text{Pb}(\text{Co}_{1/3}\text{Nb}_{2/3})\text{O}_3$ for different pressures. The inset shows the pressure dependence of the critical exponent γ and the Curie-like constant C' estimated from equation (1).

(measured at 1KHz) for $\text{Pb}(\text{Mg}_{1/3}\text{Nb}_{2/3})\text{O}_3$, and 1.76 and 2.0×10^7 (measured at 1KHz) for $\text{Pb}(\text{Zn}_{1/3}\text{Nb}_{2/3})\text{O}_3$ with DPT, respectively¹⁵⁾. The value of C' for ferroelectrics with DPT has been known to be much larger than that for ferroelectrics with the sharp phase transition¹⁵⁾. Such a decrease in both γ and C' with p corresponds to a decrease in the phase transition diffuseness of $\text{Pb}(\text{Co}_{1/3}\text{Nb}_{2/3})\text{O}_3$ with pressure. Figure 6 shows the polarization (P)-electric field (E) hysteresis loop at -117°C at atmospheric pressure with an AC amplitude of 30.0 KVcm^{-1} applied along $[100]$ for the single crystal. It was difficult to apply a strong field to obtain well-saturated P-E hysteresis loops without breaking the specimen, because of the increase in the coercive field E_c with decreasing T at tempera-

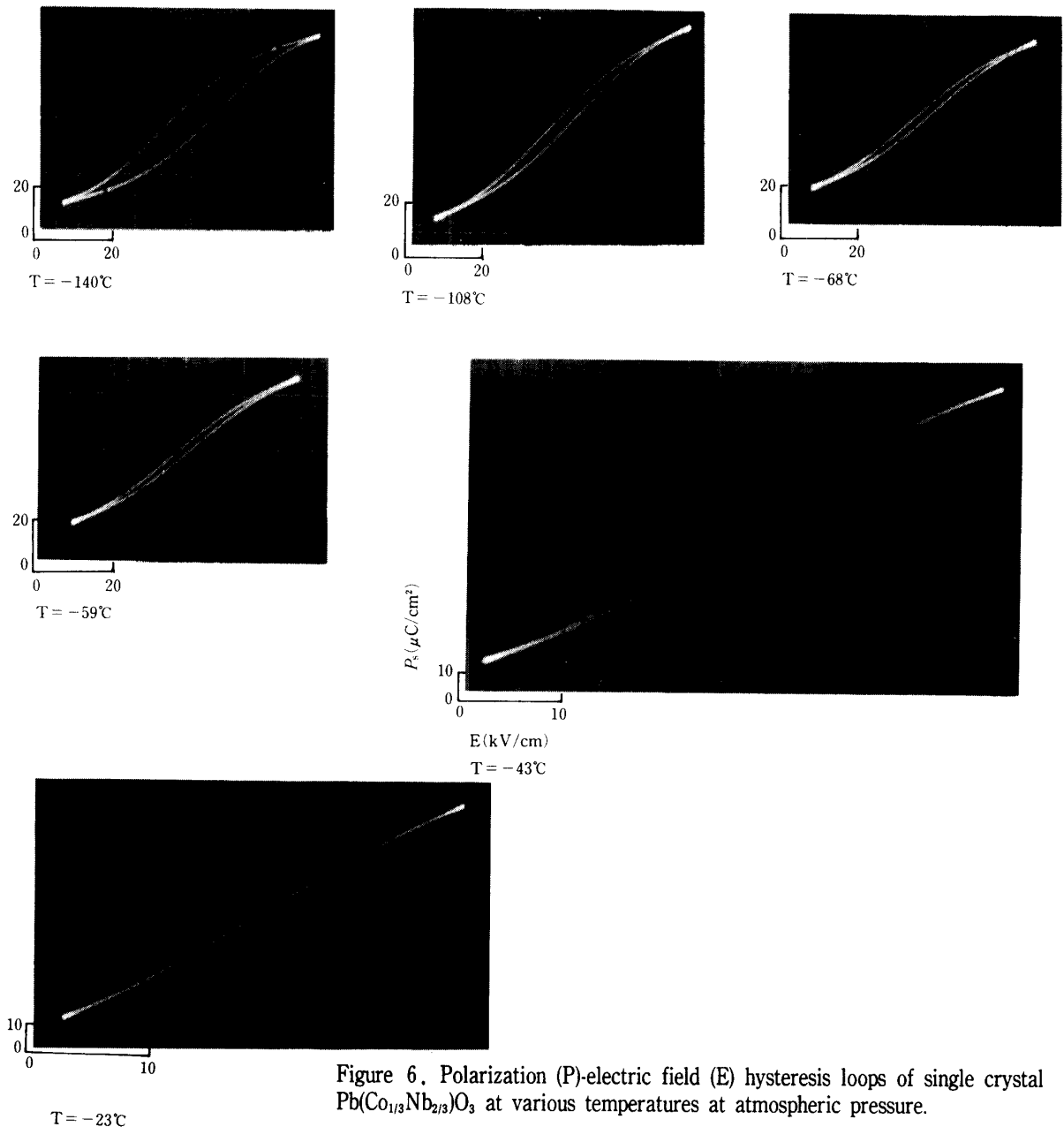


Figure 6. Polarization (P)-electric field (E) hysteresis loops of single crystal $\text{Pb}(\text{Co}_{1/3}\text{Nb}_{2/3})\text{O}_3$ at various temperatures at atmospheric pressure.

tures far below the transition point T_t and because of the increase in the conductivity with increasing T at temperatures near T_t . P-E hysteresis loops as shown in figure 6 is a better-defined saturation than that observed by Bokov et al²⁾. Figures 7(a) and (b) show the temperature dependence of the spontaneous polarization P_s and the coercive field E_c obtained from P-E hysteresis loop at atmospheric pressure, respectively. The value of P_s decreases slowly with increasing temperature. The temperature dependence of the coercive field E_c is similar to that of P_s .

Figure 9-16 are calculated curves that show $\text{Pb}(\text{Co}_{1/3}\text{Nb}_{2/3})\text{O}_3$ characteristics for various parameters such as the standard deviation σ , the Curie constant C , the difference Δ between the local Curie temperature θ and the Curie-Weiss temperature $\theta_0 = \theta'_0$ and the mean local Curie temperature θ_{av} .

Figure 9 shows the effect of the standard deviation σ on the T - ϵ' characteristic (calcu-

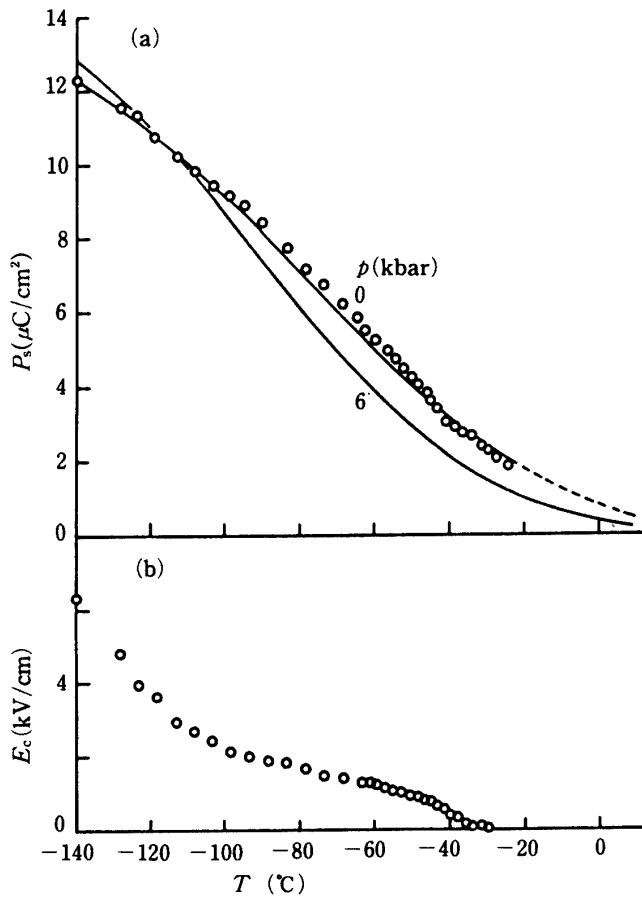


Figure 7. Temperature dependence of (a) the spontaneous polarization P_s (full curves are calculated values) and (b) the coercive field E_c of single crystal $\text{Pb}(\text{Co}_{1/3}\text{Nb}_{2/3})\text{O}_3$ for different pressures.

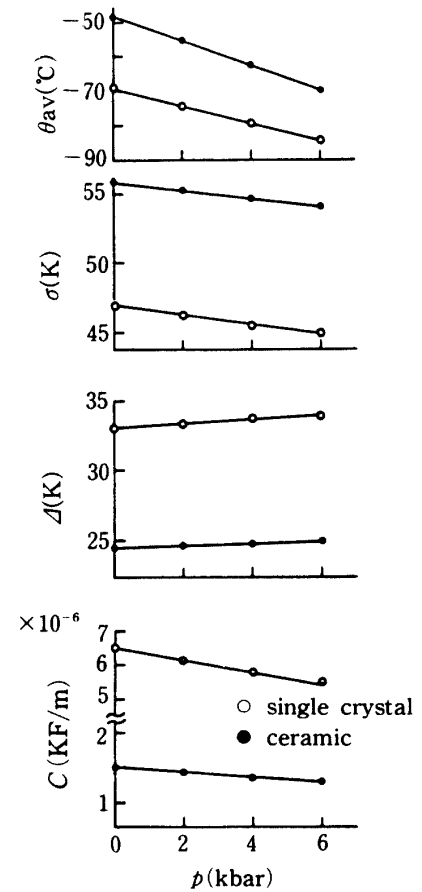


Figure 8. Pressure dependence of the mean Curie temperature θ_{av} , the standard deviation σ , the difference between the Curie temperature and the Curie-Weiss temperature Δ and the Curie constant C for the ceramic and the single crystal.

lated). As σ decreases, the T vs. ϵ'_r curve becomes sharper and $\epsilon'_{r\max}$ is larger and T_m shifts towards lower temperatures. Figure 10 shows the effect of σ on the T - P_s characteristic. As σ decreases, P_s increases in the ferroelectric phase, while P_s decreases in the paraelectric phase. Figure 11 shows the effect of the Curie constant C on the T - ϵ'_r characteristic. As C increases, $\epsilon'_{r\max}$ increases, but T_m remains constant. Figure 12 shows the effect of the Curie constant on the T - P_s characteristic. As C increases, P_s decreases. Figure 13 shows the effect of the difference Δ between the local Curie temperature and Curie-Weiss temperature on the T - ϵ'_r characteristic. As Δ increases, $\epsilon'_{r\max}$ decreases and the temperature that gives $\epsilon'_{r\max}$ shifts slightly towards higher temperatures. Figure 14 shows the effect of Δ on the T - P_s characteristic. As Δ increases, P_s increases slightly. Figure 15 shows the effect of the mean local Curie temperature θ_{av} on the T - ϵ'_r characteristic. As θ_{av} increases, T_m increases and $\epsilon'_{r\max}$ keeps constant. Figure 16 shows the effect of θ_{av} on the T - P_s characteristic. As θ_{av} increases, the T - P_s curve shifts towards higher temperatures.

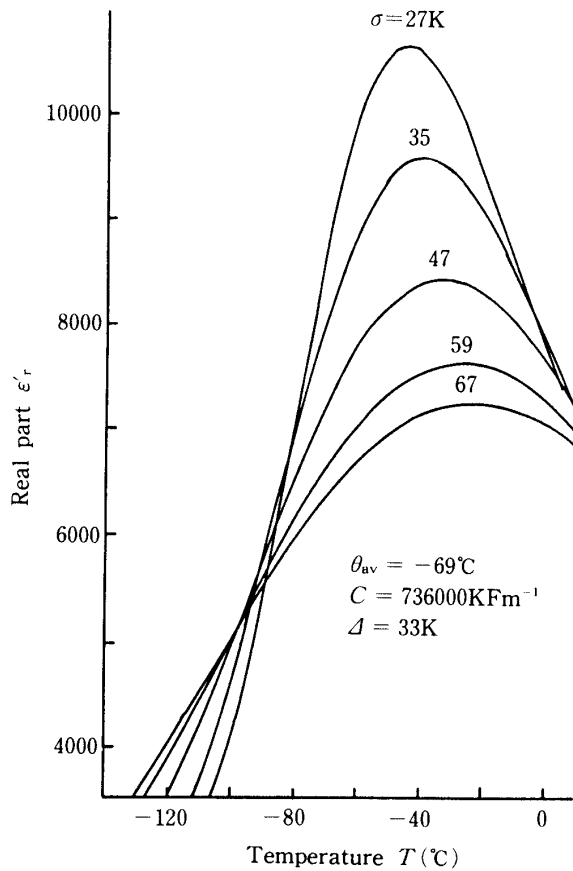


Figure 9. Effect of the standard deviation σ on the T - ϵ'_r characteristic.

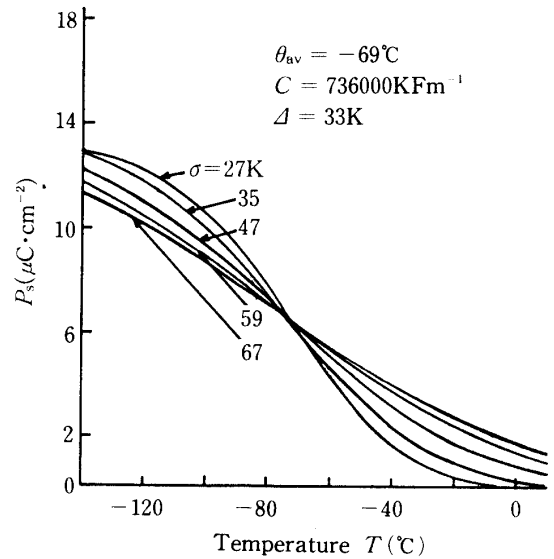


Figure 10. Effect of the standard deviation σ on the T - P_s characteristic.

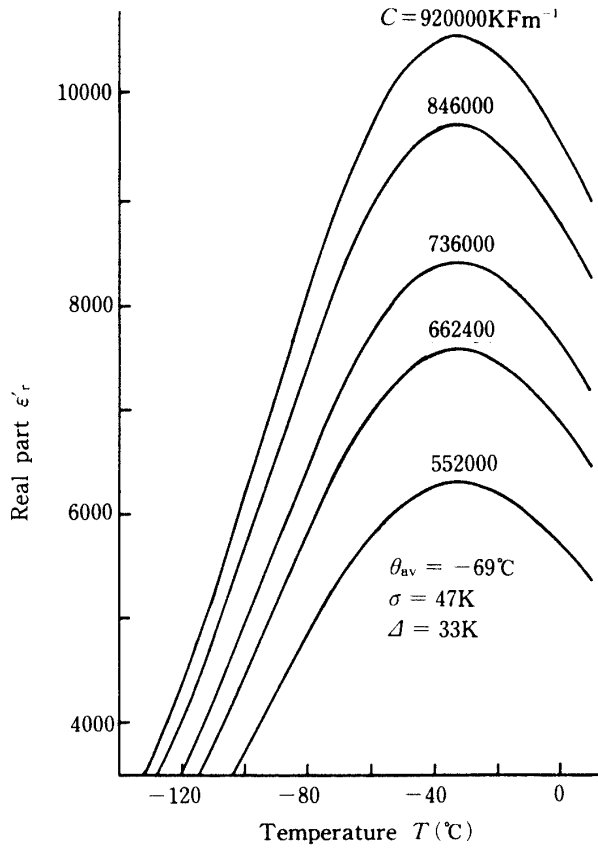


Figure 11. Effect of the Curie constant C on the T - ϵ'_r characteristic.

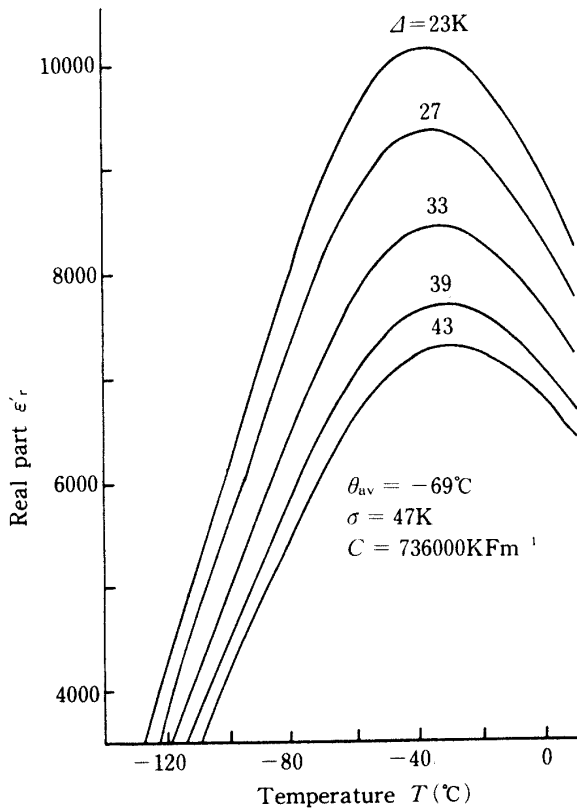


Figure 13. Effect of the difference Δ between the local Curie temperature and Curie-Weiss temperature on the T - ϵ'_r characteristic ($\theta'_0 = \theta_0$).

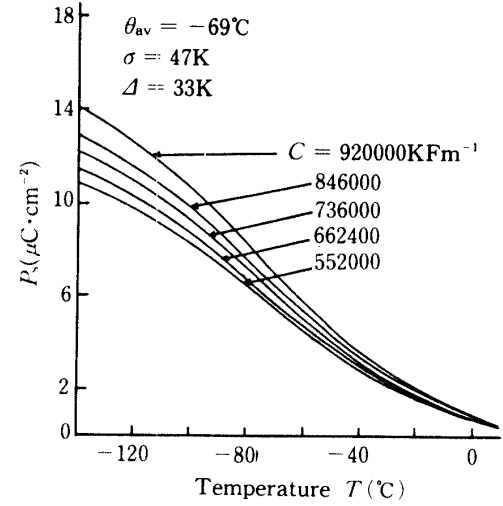


Figure 12. Effect of the Curie constant C on the T - P_s characteristic.

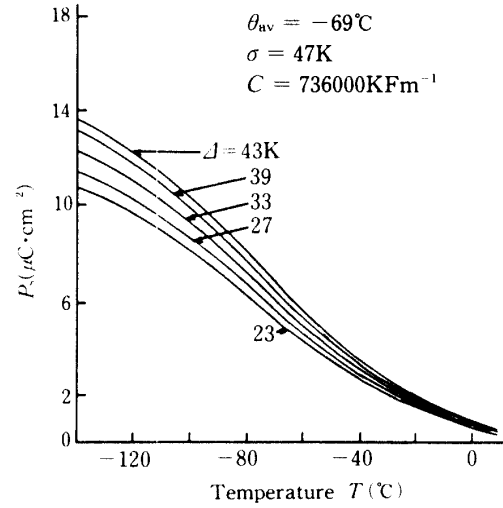


Figure 14. Effect of the difference Δ between the local Curie temperature and Curie-Weiss temperature on the T - P_s characteristic ($\theta'_0 = \theta_0$).

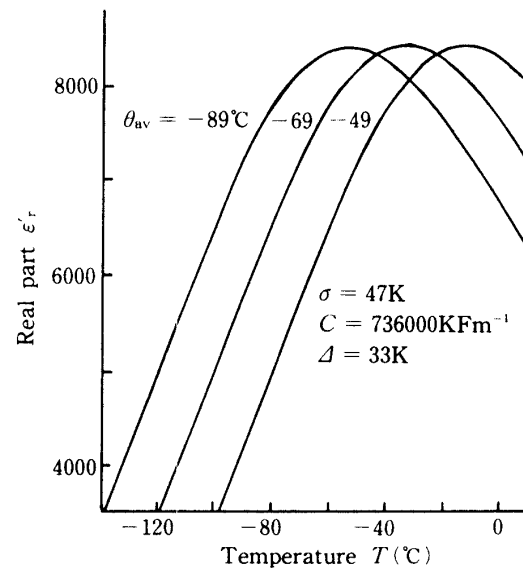


Figure 15. Effect of the mean local Curie temperature θ_{av} on the T - ϵ'_r characteristic.

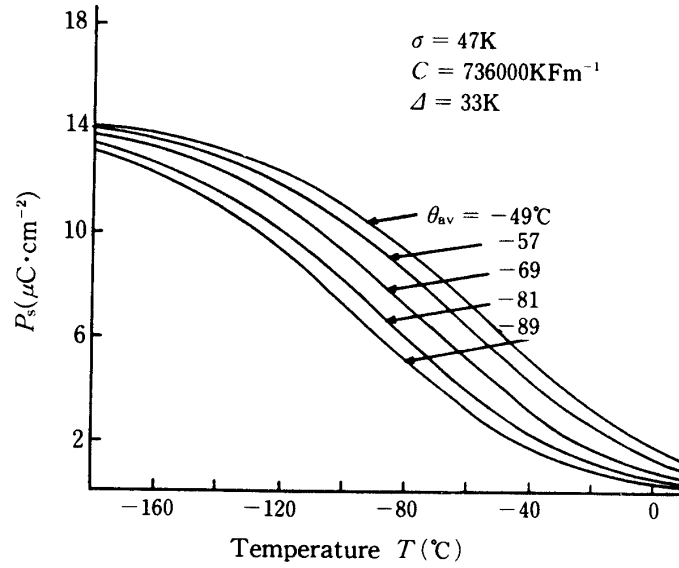


Figure 16. Effect of the mean local Curie temperature θ_{av} on the T- P_s characteristic.

4. Discussion

$\text{Pb}(\text{Co}_{1/3}\text{Nb}_{2/3})\text{O}_3$ is a ferroelectric with DPT. According to a microscopic composition fluctuation model^{14,16)}, the statistical composition fluctuation in a complex perovskite produces microscopic regions. Each of these microvolume regions (Känzig regions) has somewhat different Curie temperature and similar unbroadened dielectric characteristics. The overall properties result from the distribution of the local Curie temperatures of these individual microvolumes. Such a distribution of the local Curie temperature θ has been known to be described by a Gaussian-type distribution around a mean value of the local Curie temperature θ_{av} with a standard deviation σ describing the intensity of DPT^{14,16)}.

$$f(\theta) = (2\pi\sigma^2)^{-1/2} \exp[-(\theta - \theta_{av})^2 / 2\sigma^2] \quad (2)$$

The mean reciprocal permittivity ϵ^{-1} and the mean spontaneous polarization P_s are represented by the following equations, respectively^{14,19)}.

$$\epsilon^{-1}(T) = \int_0^\infty \epsilon^{-1}(T, \theta) f(\theta) d\theta / \int_0^\infty f(\theta) d\theta \quad (3)$$

and

$$P_s(T) = \int_0^\infty P_s(T, \theta) f(\theta) d\theta / \int_0^\infty f(\theta) d\theta \quad (4)$$

The reciprocal permittivity and the spontaneous polarization of each microregion are given by the following equations, respectively, using the expression for the free energy F

$$F = \frac{(T - \theta'_0)}{2C} P^2 + \frac{1}{4} \xi P^4 + \frac{1}{6} \zeta P^6$$

where $\theta'_0 = \theta_0 - Cgp$, C is the Curie constant, g is the hydrostatic electrostrictive constant, θ_0 is the Curie-Weiss temperature, and ξ and ζ are phenomenological constants^{10,17,18}.

$$\left. \begin{aligned} \epsilon^{-1}(T, \theta) &= \frac{-4(T - \theta'_0)}{C} + \frac{16\Delta}{3C\xi} \left[1 + \left(1 - \frac{3(T - \theta'_0)}{4\Delta} \right)^{1/2} \right] \quad (T < \theta) \\ \epsilon^{-1}(T, \theta) &= \frac{T - \theta'_0}{C} \quad (T \geq \theta) \end{aligned} \right\} \quad (5)$$

and

$$\left. \begin{aligned} P_s(T, \theta)^2 &= \frac{-8\Delta}{3C\xi} \left[1 + \left(1 - \frac{3(T - \theta'_0)}{4\Delta} \right)^{1/2} \right] \quad (T < \theta) \\ P_s(T, \theta) &= 0 \quad (T \geq \theta) \end{aligned} \right\} \quad (6)$$

where

$$\Delta = \theta - \theta'_0 = 3C\xi^2/16\zeta$$

The temperature dependence of the mean permittivity and the mean spontaneous polarization calculated from equations (2)-(6) with a computer are shown as full lines in figures 2(a), 3(a) and 7(a) using $\xi = -1.8 \times 10^9 \text{ m}^5 \text{F}^{-1} \text{C}^{-2} < 0$. Here a first order transition for each microregion is assumed^{10,17}. The calculation was done by means of a parameter estimation method which minimizes the error between measured points and calculated ones from equations (2)-(6) by a suitable variation of the parameter involved. Good agreement is obtained between the observed values and the calculated ones. The pressure dependence of the parameters used in calculating ϵ and P_s for the single crystal and the ceramic are shown in figure 8. The measured values of $dT_m/dp = -3.0 \text{ Kkbar}^{-1}$ for the crystal and -3.5 Kkbar^{-1} for the ceramic were used as the values of $d\theta_{av}/dp$. The value of the standard deviation σ describing the intensity of DPT is 47K for the single crystal and 55.4K for the ceramic at atmospheric pressure. These values are comparable with values of 39K for $\text{Pb}(\text{Mg}_{1/3}\text{Nb}_{2/3})\text{O}_3$ ¹⁶ and 37K for $\text{Pb}(\text{Fe}_{2/3}\text{W}_{1/3})\text{O}_3$ ⁹. The value of σ decreases with a pressure coefficient $d\sigma/dp = 0.33 \text{ Kkbar}^{-1}$ for the single crystal and $d\sigma/dp = 0.30 \text{ Kkbar}^{-1}$ for the ceramic with increasing p as shown in figure 8, and the phase transition of $\text{Pb}(\text{Co}_{1/3}\text{Nb}_{2/3})\text{O}_3$ becomes less diffused with increasing p . This result agrees with the decrease in the phase transition diffuseness with p , corresponding to the decrease in the critical exponent γ with p in § 3. The value of C estimated at atmospheric pressure is $6.52 \times 10^{-6} \text{ K Fm}^{-1}$ for the single crystal and $1.50 \times 10^{-6} \text{ K Fm}^{-1}$ for the ceramic. The former value is comparable with the value of $4.16 \times 10^{-6} \text{ K Fm}^{-1}$ for single crystal $\text{Pb}(\text{Zn}_{1/3}\text{Nb}_{2/3})\text{O}_3$ ¹⁹. The value of C for both samples decrease slightly with increasing p as shown in figure 8. On the other hand, the value of Δ for both samples increases gradually with increasing p , and this fact is expected from the decreases in σ with increasing p . The hydrostatic electrstrictive constant g is estimated to be $0.46 \times 10^{-2} \text{ m}^4 \text{C}^{-2}$ for the single

crystal and $2.31 \times 10^{-2} \text{ m}^4 \text{C}^{-2}$ for the ceramic from the relation

$$dT_i/dp \text{ (or } d\theta_{av}/dp) = -Cg$$

using the above value of C . This value of g is compared with the value of $1.74 \times 10^{-2} \text{ m}^4 \text{C}^{-2}$ for $\text{Pb}(\text{Fe}_{2/3}\text{W}_{1/3})\text{O}_3$ ⁹⁾. It is confirmed in figure 7 that the calculated value of P_s at -110°C increases with increasing pressure, and that the phase transition diffuseness decreases with increasing pressure. These results agree with the decrease in the critical exponent γ with increasing pressure.

5. Summary

The dielectric properties such as the real ϵ' and imaginary ϵ'' parts of the complex permittivity and the spontaneous polarization P_s of single crystal and ceramic $\text{Pb}(\text{Co}_{1/3}\text{Nb}_{2/3})\text{O}_3$ with the diffuse phase transition (DPT) were measured under various pressures up to 6kbar. The value of ϵ' shows a broad maximum at a temperature T_m (mean Curie temperature). The value of the critical exponent γ for the logarithmic plots of the reciprocal ϵ' against the reduced temperatures above the transition point T_i (or mean Curie temperature θ_{av}) is 1.85 for the crystal. With increasing pressure p , the values of γ and T_i decrease with a pressure coefficient $dT_i/dp \simeq -3.5 \text{ Kkbar}^{-1}$ for the ceramic and -3.0 Kkbar^{-1} for the crystal, and the sharpening of the maximum in ϵ' or ϵ'' increases. The temperature and pressure dependence of ϵ' and P_s is explained in terms of a phenomenological theory using statistical treatments based on a Gaussian distribution of the local Curie temperature. The value of the standard deviation σ describing the intensity of DPT is 56K for the ceramic and 47K for the crystal, and decreases with increasing pressure. The phase transition becomes less diffused with increasing p . The values of the Curie constant and the hydrostatic electrostrictive constant are estimated as $6.52 \times 10^{-6} \text{ Kfm}^{-1}$ and $0.46 \times 10^{-2} \text{ m}^4 \text{C}^{-2}$ for the crystal, and $1.51 \times 10^{-6} \text{ Kfm}^{-1}$ and $2.31 \times 10^{-2} \text{ m}^4 \text{C}^{-2}$ for the ceramic, respectively.

References

- 1) G. A. Smolenskii : *Ferroelectrics* **53** (1984) 129.
- 2) V. A. Bokov and L. A. Myl'nikova : *Sov. Phys.-Solid State* **2** (1961) 2428.
- 3) B. A. Malkov and Yu. N. Venetsev : *Izv. Akad. Nauk SSSR, Neorg. Mater.* **13** (1977) 1468.
- 4) V. D. Sal'niov, Yu. S. Kuz'minov and Yu. N. Venetsev : *Izv. Akad. Nauk SSSR, Neorg. Mater.* **7** (1971) 1277.
- 5) O. N. Razumovskaya, R. U. Devlikanova, I. N. Belyaev and T. B. Tokmyanina : *Izv. Akad. Nauk SSSR, Neorg. Mater.* **11** (1975) 1260.
- 6) Yu. E. Roginskaya, Yu. N. Venetsev and G. S. Zhdanov : *Sov. Phys. JETP* **21** (1965) 817.
- 7) N. Setter and L. E. Cross : *J. Appl. Phys.* **51** (1980) 4356.
- 8) N. Yasuda, S. Fujimoto, K. Tanaka and T. Hachiga : *J. Phys. D : Appl. Phys.* **17** (1984) 2069.

- 9) N. Yasuda, S. Fujimoto and K. Tanaka : J. Phys. D : Appl. Phys. **18** (1985) 1909.
- 10) S. Fujimoto and N. Yasuda : Japan. J. Appl. Phys. **15** (1976) 595.
- 11) N. Setter and L. E. Cross : J. Cryst. Growth **50** (1980) 555.
- 12) N. Yasuda, S. Fujimoto, M. Okamoto, H. Simizu, K. Yoshino and Y. Inuishi : Phys. Rev. B **20** (1979) 2755.
- 13) N. Setter and L. E. Cross : Phys. Stat. Sol. (a) **61**, (1980) K71.
- 14) R. Clarke and J. C. Burfoot : Ferroelectrics **8** (1974) 505.
- 15) K. Uchino and S. Nomura : Ferroelectrics Lett. **44** (1982) 55.
- 16) V. V. Kirillov and V. A. Isupov : Ferroelectrics **5** (1973) 3.
- 17) S. Fujimoto, N. Yasuda, A. Kawamura and T. Hachiga : J. Phys. D : Appl. Phys. **17** (1984) 1019.
- 18) G. A. Samara : Advances in High Pressure Research vol. 3, ed., R S Bradly (New York : Academic, 1969).
- 19) J. Kuwata, K. Uchino and S. Nomura : Ferroelectrics **22** (1979) 863.